PNAS RESEARCH ARTICLE | CELL BIOLOGY OPEN ACCESS

Following phospholipid transfer through the $OmpF_3$–MlaA–MlaC lipid shuttle with native mass spectrometry

Carla Kirschbaum[a,b], Jack L. Bennett[a,b], Qiaoyu Tian[c], Navoneel Sen[a,b], Iain P. S. Smith[d], Di Wu[a,b], Justin L. P. Benesch[a,b], Syma Khalid[d], Georgia Isom[c], and Carol V. Robinson[a,b,1]

Affiliations are included on p. 10.

Edited by Natalie Ahn, University of Colorado Boulder, Boulder, CO; received September 30, 2024; accepted March 4, 2025

The maintenance of lipid asymmetry (Mla) system in gram-negative bacteria transfers phospholipids between the outer and inner membrane to maintain the outer membrane asymmetry. Misplaced phospholipids are extracted from the outer leaflet of the outer membrane by MlaA, transferred to the periplasmic lipid transporter MlaC, and shuttled to the inner membrane. We set out to investigate the lipid transfer between MlaA and MlaC using native mass spectrometry, with the aim of determining the lipid preferences of MlaC and whether MlaA preselected lipids for MlaC. First, we characterized the lipids that copurified with overexpressed MlaC, phosphatidylglycerol (PG), and phosphatidylethanolamine (PE), and following delipidation noted a headgroup-independent enrichment of cyclopropane lipids. Under native expression conditions, we found that PG is three-fold enriched on MlaC compared to its abundance in the membrane. Next, we isolated and characterized $OmpF_3$–MlaA complexes and demonstrated their ability to enhance loading of delipidated MlaC with bacterial and nonbacterial phospholipids. We then captured the intact ternary lipid shuttle ($OmpF_3$–MlaA–MlaC) and demonstrated that PG dissociates this transient complex, releasing lipid-bound MlaC. Together our results point to a high population of endogenous PG on periplasmic MlaC, which likely arises from disassembly of the lipid shuttle to maintain lipid asymmetry for cell viability.

maintenance of lipid asymmetry system | lipid transporters | membrane proteins | phospholipids | native mass spectrometry

Significance

The outer membrane asymmetry of gram-negative bacteria is actively maintained by the Mla system. Here, we use native mass spectrometry to study the loading of phospholipids onto the lipid transporter MlaC, via the outer membrane protein complex $OmpF_3$–MlaA. We demonstrate that $OmpF_3$–MlaA significantly increases lipid loading by recruiting phospholipids and *apo* MlaC. We capture the ternary $OmpF_3$–MlaA–MlaC lipid shuttle and show that phosphatidylglycerol (PG) binding induces dissociation of this transient protein complex. Unexpectedly, we find a three-fold enrichment of PGs on MlaC endogenously expressed in *Escherichia coli*, consistent with an enhanced flux of PGs through the $OmpF_3$–MlaA–MlaC lipid shuttle. More generally, our study elucidates molecular details of a pivotal process in gram-negative bacteria that ensures membrane integrity and protection against antibiotics.

The cell envelope of gram-negative bacteria has a unique and complex architecture (1). It is composed of two distinct membranes separated by an aqueous periplasmic space that is spanned by a thin peptidoglycan layer. The outer membrane is the first line of defense against the intrusion of noxious substances. Its outer leaflet consists almost entirely of dense, negatively charged lipopolysaccharides (LPS), which form an effective permeability barrier. The inner leaflet of the outer membrane is mainly composed of phospholipids, including 80% phosphatidylethanolamine (PE), 15% phosphatidylglycerol (PG), and 5% cardiolipin (CDL) (2). In contrast, the inner membrane contains phospholipids in both leaflets with a slightly lower PE/PG ratio (70/25%) than the outer membrane.

The integrity of the asymmetric outer membrane is crucial for the survival of gram-negative bacteria. If phospholipids are enriched in the outer leaflet, they can form permeable patches that make bacteria more susceptible to harmful toxins including antibiotics (3). Therefore, gram-negative bacteria have evolved a protein machinery that removes misplaced phospholipids from the outer leaflet of the outer membrane: the maintenance of lipid asymmetry (Mla) system (4). The Mla system extracts phospholipids from the LPS leaflet, transports them through the periplasm in a retrograde fashion (5), and integrates them back into the inner cell membrane (Fig. 1) (6, 7).

The Mla system comprises proteins in the outer membrane, periplasm, and inner membrane. The outer membrane component is MlaA, a monomeric alpha-helical lipoprotein that associates with the outer membrane porins OmpC and OmpF (8). Both homotrimeric porins form virtually identical complexes with MlaA (9), which is thought to bind at their subunit interfaces (10). MlaA protrudes into the outer leaflet of the outer membrane and contains a central channel, enabling the protein to extract phospholipids from the outer leaflet while preventing access of phospholipids from the inner leaflet into the channel (9, 10). Phospholipid binding to MlaA has not been observed previously (1). As a diffusion channel, MlaA should only transiently be associated with lipids and effectively transfer them to the phospholipid transporter MlaC (6).

MlaC is the periplasmic component of the Mla system that shuttles phospholipids from the outer to the inner membrane. In line with its role as a phospholipid transporter, MlaC exhibits high affinity for phospholipids and is known to copurify with PE and PG (11–13).

Author contributions: C.K., J.L.B., Q.T., S.K., G.I., and C.V.R. designed research; C.K., J.L.B., Q.T., N.S., I.P.S.S., and D.W. performed research; C.K., J.L.B., N.S., and I.P.S.S., and J.L.P.B. analyzed data; and C.K., J.L.B., and C.V.R. wrote the paper.

The authors declare no competing interest.

This article is a PNAS Direct Submission.

[1]To whom correspondence may be addressed. Email: carol.robinson@chem.ox.ac.uk.

This article contains supporting information online at https://www.pnas.org/lookup/suppl/doi:10.1073/pnas.2420041122/-/DCSupplemental.

Published April 1, 2025.

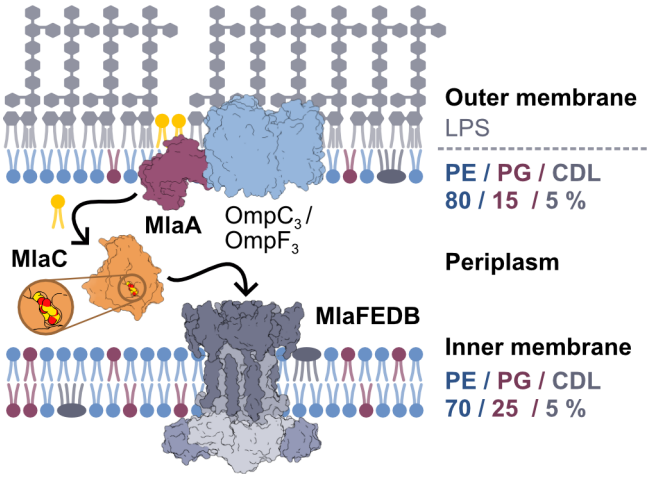

Fig. 1. Schematic overview of the Mla system. Misplaced phospholipids (yellow) are extracted from the outer leaflet of the outer membrane by MlaA, which is associated with $OmpC_3$ or $OmpF_3$. The lipids are transferred to MlaC in the periplasm and delivered to MlaFEDB in the inner membrane. The typical distribution of phosphatidylethanolamine (PE), phosphatidylglycerol (PG), and cardiolipin (CDL) in the inner and outer membranes of *Escherichia coli* is shown; LPS = lipopolysaccharide. The peptidoglycan layer is omitted for visibility.

Escherichia coli (*E. coli*) MlaC has also been previously reported to copurify with CDL based on thin layer chromatography (TLC);(12) however, its binding pocket is small compared to MlaC homologs that can accommodate four acyl chains (14, 15). Moreover all crystal structures of *E. coli* MlaC only contain diacylglycerol phospholipids, making CDL binding less likely (14). In crystal structures of phospholipid-bound MlaC, the acyl chains are buried in the binding pocket, while the phospholipid headgroup is solvent-exposed and makes only minor contact with the protein (14).

How then is MlaC loaded with phospholipids? Molecular dynamics (MD) simulations suggest that *apo* MlaC does not readily sample the open conformation, and spontaneous loading of *apo* MlaC by passive diffusion of phospholipids is negligible (12). Moreover, it was shown by cross-linking experiments, mutagenesis, and in silico modeling that for loading and unloading of phospholipids, both MlaA and the MlaD subunit of MlaFEDB interact with MlaC close to its phospholipid binding pocket (11, 16).

The ABC transporter MlaFEDB is the inner membrane component of the Mla system which drives phospholipid transfer from MlaC to the inner membrane (17). MlaC relays its phospholipid cargo to the MlaD subunit of the MlaFEDB complex in an ATP-dependent manner (5, 18). ATP is required to drive retrograde lipid transfer because MlaC has a higher phospholipid affinity than MlaD (11, 12).

The mechanism of active phospholipid transfer between MlaC and the MlaFEDB complex has been studied extensively (5, 11, 12, 18–20). However, little is known about the transfer of phospholipids, or any preferences thereof, from MlaA to MlaC at the outer membrane, a process which is thought to be affinity-driven (21). Recent studies describe the structure of a disulfide-trapped $OmpC_3$–MlaA–MlaC complex(22) and observe macroscopic lipid flow from MlaA to MlaFEDB via MlaC in a proteoliposome transport assay (5). However, these studies did not investigate explicitly the lipid transfer or lipid preferences between MlaA and MlaC. Therefore, the lipid specificity and the role of MlaA in the loading efficiency and selection in this lipid transfer remains unknown.

In this study, we follow the MlaA-mediated transfer of phospholipids to *E. coli* MlaC using native mass spectrometry (MS). We demonstrate that $OmpF_3$–MlaA simultaneously recruits *apo* MlaC and phospholipids, thus greatly enhancing lipid transfer to MlaC in solution. We capture the ternary $OmpF_3$–MlaA–MlaC complex in a lipid-free environment and show that it dissociates in the presence of lipids. We further show that MlaA transfers different diacylglycerol phospholipids but that CDL does not bind to MlaC under these conditions. Despite similar loading efficiencies for the *E. coli* phospholipids PE and PG in vitro, we note a significant enrichment of PG over PE in overexpressed and endogenously expressed MlaC and discuss possible implications of this observation.

Results

***E. coli* MlaC Copurifies with the Major Endogenous PE and PG Lipids.** To investigate the lipid transporter MlaC and characterize its endogenous phospholipids, we coexpressed MlaC and MlaA in *E. coli* and analyzed purified MlaC using native MS. In positive mode, we observed both *apo* and lipid-bound MlaC monomers in three major charge states (8 to 10+), and a small fraction of dimers (12 to 14+) (Fig. 2*A*). SDS-PAGE and native MS confirmed that the MlaC signal peptide was completely cleaved, which suggests its exclusive localization within the periplasm (*SI Appendix*, Fig. S1). More than 95% of purified MlaC was observed bound to phospholipids; the peak pattern was complex, indicating promiscuous binding to a variety of distinct lipid species. To identify the bound phospholipids, we isolated lipid-bound MlaC (9+) in the mass spectrometer and subjected these selected ions to collision-induced dissociation (CID). At low collision energies, product ions were released from MlaC with masses consistent with protonated PE, sodiated PE, and sodiated PG (Fig. 2*B*). CDLs were not detected.

To identify the PE and PG lipids that copurify with MlaC, we reisolated and subsequently activated each released lipid using higher-energy collisional dissociation (HCD) in both positive and negative modes. The resulting fragmentation spectra (MS^3) in positive ion mode revealed the lipid class (headgroup), whereas the fatty acids were observed as carboxylate anions in negative ion mode. The relative intensities of the carboxylate ions were used to assign the *sn*-positions of the fatty acids in the predominant isomer (23). We observed a significant amount of cyclopropane (cy) lipids, which are known to increase in the stationary growth phase and under stress conditions, such as protein overexpression (*SI Appendix*, Fig. S2) (2). Our analysis revealed that the major lipids bound to MlaC were PG and PE with 32:1, 33:1, 34:2, 34:1, 35:2, and 36:2 acyl chains containing mainly 16:1, 16:0, 17:1(cy), 18:1, and 19:1(cy) fatty acids (Table 1). These assignments correspond to the most abundant lipids previously identified in an *E. coli* lipid extract (24). We also confirmed that the composition of lipids that copurify with MlaC remained constant across three replicate protein expressions (*SI Appendix*, Fig. S2). Overall, multistage native MS allowed us to reproducibly identify all major PE and PG lipids that copurify with MlaC, revealing molecular details and information on their relative abundances.

Successive Delipidation of MlaC Retains Phospholipids with Specific Acyl Chains. To obtain *apo* MlaC for subsequent loading experiments and investigate lipid preferences, we removed the endogenous lipids copurifying with MlaC. Briefly, we treated MlaC with the delipidating detergent octyl-β-glucoside (OG; 2%) for 1 to 24 h (*SI Appendix*, Fig. S3). After 24 h, we achieved almost complete delipidation (Fig. 2*C*). Throughout the delipidation experiment, the PE/PG ratio gradually increased from 35 ± 1 to 54 ± 1% (based on intensities in the MS^2 spectra), suggesting stronger retention of PE lipids. Furthermore, close

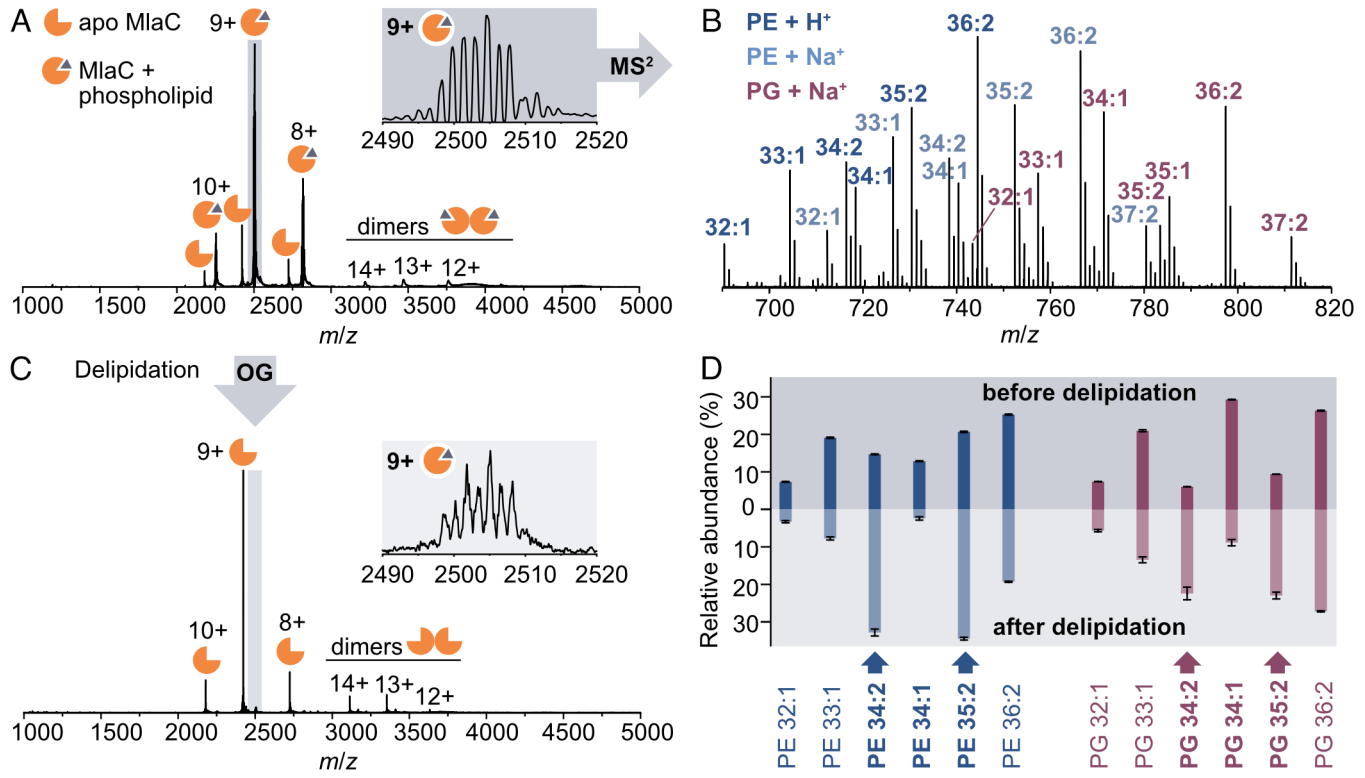

Fig. 2. Characterization of phospholipids copurifying with MlaC. (*A*) Native mass spectrometry demonstrates that the majority of purified MlaC is phospholipid-bound. (*B*) Phospholipids were released from MlaC and identified by tandem mass spectrometry (MS^2). They comprise PE and PGs. (*C*) Endogenous phospholipids were removed by octyl-β-glucoside (OG), resulting in almost complete delipidation. (*D*) Comparison between phospholipids bound to MlaC, before and after delipidation, shows headgroup-independent enrichment of cyclopropane lipids (34:2 and 35:2). PE and PG are plotted individually, and error bars represent the SD between triplicate delipidation experiments.

examination of the lipids that remained bound to MlaC after delipidation revealed clear differences in the acyl chain profile (Fig. 2*D*). In particular, 34:2 and 35:2 lipids were retained to a great extent, while 34:1 lipids were largely depleted after delipidation. This trend was consistent for both PE and PG, in agreement with the fact that most of the protein–lipid contacts are established by the acyl chains rather than the lipid headgroup (14).

Table 1. Assignment of the most abundant phospholipids detected in the positive mode MS^2 spectrum of lipid-bound MlaC (*cf.* Fig. 2*B*). Minor acyl chains make up ≤20% of the respective lipid

Lipid		*m/z*	Major acyl chains	Minor acyl chains
PE 32:1	$M+H^+$	690.5	16:0/16:1	14:0/18:1
	$M+Na^+$	712.5		15:0/17:1(cy)
PE 33:1	$M+H^+$	704.5	16:0/17:1(cy)	15:0/18:1
	$M+Na^+$	726.5		
PE 34:2	$M+H^+$	716.5	18:1/16:1	17:1/17:1(cy)
	$M+Na^+$	738.5		
PE 34:1	$M+H^+$	718.5	16:0/18:1	
	$M+Na^+$	740.5		
PE 35:2	$M+H^+$	730.5	18:1/17:1(cy)	16:1_19:1(cy)
	$M+Na^+$	752.5		
PE 36:2	$M+H^+$	744.6	18:1/18:1	17:1(cy)_19:1(cy)
	$M+Na^+$	766.5		
PG 32:1	$M+Na^+$	743.5	16:0/16:1	14:0/18:1
				15:0/17:1(cy)
PG 33:1	$M+Na^+$	757.5	16:0/17:1(cy)	15:0/18:1
PG 34:2	$M+Na^+$	769.5	18:1/16:1	17:1/17:1(cy)
PG 34:1	$M+Na^+$	771.5	16:0/18:1	
PG 35:2	$M+Na^+$	783.5	18:1/17:1(cy)	16:1_19:1(cy)
PG 35:1	$M+Na^+$	785.5	16:0/19:1(cy)	
PG 36:2	$M+Na^+$	797.5	18:1/18:1	17:1_19:1(cy)
PG 37:2	$M+Na^+$	811.6	18:1/19:1(cy)	

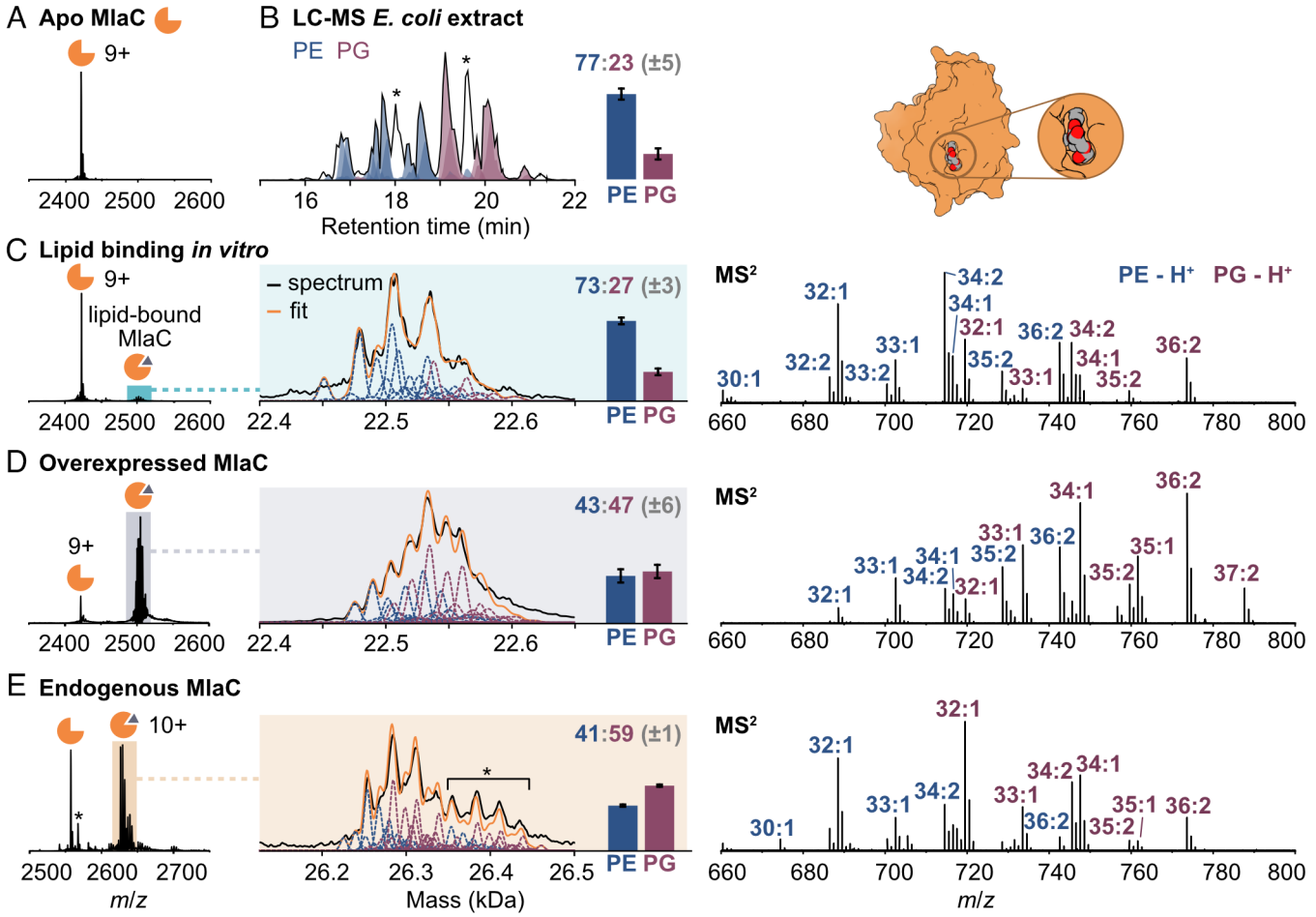

Fig. 3. Enrichment of PG on MlaC extracted from *E. coli*. (*A*) Mass spectrum of delipidated MlaC before incubation with lipids. (*B*) LC-MS(−) analysis of total lipid extract from MlaC-expressing *E. coli*. Asterisks indicate phospholipid standards in the chromatogram [PC 15:0_18:1(d7) and PG 15:0_18:1(d7)]. (*C*) Mass spectrum of delipidated MlaC incubated with *E. coli* lipids in vitro. The resulting lipid binding pattern is centered around a lower mass than the lipids copurifying with overexpressed MlaC (*D*). The lipid-bound states in the deconvoluted mass spectra were fitted with gaussians for relative PE/PG quantification. The observed mass shift arises from a substantial enrichment of heavier PG over PE in MlaC extracted from cells, also reflected in the corresponding MS^2 spectra. (*E*) Lipids copurifying with endogenously tagged MlaC show two distributions shifted by 100 Da, which corresponds to a covalent modification on the Strep tag (indicated by asterisks). The lipid binding pattern is clearly enriched in short-chain PG.

We then searched for structural features in the acyl chains that could explain differences in the retention of phospholipids upon delipidation. We noted that the lipids which are most retained after treatment with OG (PE/PG 34:2 and 35:2) combine two structural features: They contain cyclopropane fatty acids and no saturated chains. The presence of a saturated lipid chain leads to increased removal of the corresponding lipids (32:1, 33:1, 34:1) compared to those with two unsaturated or cyclopropane chains (*SI Appendix*, Fig. S3). The most drastic decrease is observed for 34:1 lipids (mainly 16:0/18:1), which could imply high solubility of the lipid in OG or a lower stability of the corresponding protein–lipid complexes. Cyclopropane chains were more tightly retained than unsaturated chains. Accordingly, 36:2 lipids (primarily 18:1/18:1) are not as strongly retained as cyclopropane-containing 34:2 and 35:2 lipids. Furthermore, if mixtures of isomers are present, delipidation increases the ratio of cyclopropane-containing isomers over unsaturated isomers, as can be seen for 34:2 and 36:2 phospholipids (*SI Appendix*, Fig. S3). Overall, our data unanimously point to enhanced retention of unsaturated and cyclopropane-containing phospholipids in MlaC upon detergent treatment.

MlaC Is Enriched in PG which Is a Minor Component of the Outer Cell Membrane. Before delipidation, we observed that MlaC copurified with a surprisingly high quantity of PG, especially given the low levels of these lipids in the outer membrane. We therefore developed an approach to quantify the relative amounts of PE and PG lipids bound to the purified protein. First, we tested whether we could reproduce the lipid profile of overexpressed MlaC in vitro by incubating the delipidated MlaC sample with a complete *E. coli* lipid extract. We obtained a total lipid extract from *E. coli* using the Bligh and Dyer method (25). Quantification of the PE and PG lipids in the extract by liquid chromatography (LC)-MS/MS yielded a total PE/PG ratio of roughly 77:23 (Fig. 3*B*). This result agrees with the typical whole-cell phospholipid content of *E. coli* (75% PE, 20% PG, 5% CDL) (1). The lipid extract was then incubated with delipidated MlaC in detergent solution (2xCMC C8E4 in 200 mM ammonium acetate) using a 150-fold excess of lipid, before removing unbound lipids by buffer exchange into ammonium acetate (Fig. 3 *A* and *C*). We found that the lipid profile differed greatly from that of overexpressed MlaC (Fig. 3*D*). The latter was shifted toward higher masses, suggesting a higher ratio of PG lipids. This was also evident through a comparison of the MS^2 spectra, where overexpressed MlaC exhibited a much higher abundance of PG lipids than MlaC loaded with the lipid extract in vitro, suggesting the enrichment of PG binding in cells.

We then developed an approach to accurately quantify the ratio of PE/PG bound to MlaC from MS^1 spectra (26). This is necessary because the peak intensities in the MS^2 spectra are not suitable

for quantification due to the different response factors of the lipids released. Briefly, we modeled the MS^1 spectra as a sum of the individual MlaC–phospholipid complexes, using the MS^2 spectra to inform the model (Fig. 3 *C* and *D*). The quantitative data revealed that the lipids released from MlaC after incubation with the *E. coli* lipid extract were strongly correlated with the composition of the lipid extract (*SI Appendix*, Fig. S4); the total PE/PG ratio remained unchanged after loading onto MlaC. Hence, we conclude that there is no preferential loading of either of the two lipid classes in solution. In contrast, for overexpressed MlaC extracted from *E. coli*, the PE/PG ratio was close to 1:1 (*SI Appendix*, Fig. S5). Such enrichment of PG is intriguing since PG only accounts for 15% of the phospholipids in the outer membrane. However, the biological significance of this enrichment remains unclear. A PE:PG ratio of ca. 1:1 has previously been reported not only for MlaC overexpressed in the periplasm (11) but also for MlaC overexpressed in the cytosol (18). In these experiments, PG cannot be loaded and unloaded via the Mla system. Furthermore, during high pressure lysis inner and outer membranes could come into contact with MlaC, facilitating lipid exchange and making it challenging to identify the true mechanistic basis for the observed PG enrichment using this approach.

To investigate the relevance of PG enrichment in a cellular context, we endeavored to purify MlaC at endogenous levels to eliminate overexpression effects. Moreover, to avoid membrane mixing during protein purification, we employed hypotonic lysis to gently lyse the outer membrane and release the periplasmic content while leaving the inner membrane intact (27). We designed an MlaC construct carrying an N-terminal Twin-Strep tag following the signal sequence, which we inserted into the *E. coli* strain BW25113 using lambda Red recombination (28) and P1 phage transduction (29). After confirming that the construct was functional (*SI Appendix*, Fig. S6), we expressed the protein in biological triplicate by growing the cells in antibiotic-free media to an OD_{600} of 0.7 to 0.8. For hypotonic lysis, we used a Tris/EDTA/sucrose buffer (30).

Native MS analysis of the resulting protein revealed a marginally higher enrichment of PG over PE (ca. 60%) than observed for overexpressed MlaC lysed under high pressure (Fig. 3*E*). The phospholipids that copurified with endogenously tagged MlaC were consistent across replicate expressions (*SI Appendix*, Fig. S7). The lipid binding pattern consisted of two identical distributions shifted by 100 Da. This binding pattern is due to a covalent modification on MlaC confirmed using native top–down MS as succinylation or methylmalonylation of the N-terminal Twin-Strep tag (6). Overall, the endogenously expressed protein tended to have shorter lipid chains and less cyclopropane modifications than those that copurified with overexpressed MlaC. This change in properties likely arises from the shorter expression time and lower cell density. We surmise that after expression at endogenous levels and gentle lysis of the outer membrane, lipids copurifying with MlaC are enriched in PG under native conditions.

MlaA Recruits Lipids to $OmpF_3$–MlaA Complexes. Given this preference for PG, we needed to determine whether the Mla loading system favors PG transfer over PE transfer. We therefore conducted lipid transfer experiments from MlaA onto delipidated MlaC, using MlaA overexpressed in *E. coli.* The native mass spectrum of purified MlaA revealed the presence of three protein complexes which, based on intact mass, we putatively assigned as $OmpF_3$, $OmpF_3$–MlaA, and $OmpF_3$–$MlaA_2$ (Fig. 4*A*). No free MlaA was observed. This is in accordance with previous observations that MlaA copurifies with outer membrane porins (OmpC or OmpF) (8). In our case, we observed MlaA solely in complex with OmpF (*SI Appendix*, Fig. S8), which is likely due to the lack of OmpC expression in *E. coli* BL21(DE3) strains (10). We also observed that the mass of MlaA is shifted by ca. 815 Da relative to its amino acid sequence. This additional mass confirms complete lipoprotein maturation, including cleavage of the signal peptide and attachment of three lipid chains (31). Specifically, we assigned the observed mass shift to the attachment of a 34:1 diacylglycerol and palmitic acid to the thiol and amino groups of the *N*-terminal cysteine, respectively (theoretical mass: 814.7 Da) (*SI Appendix*, Table S1). In addition, two minor peaks in the mass spectrum of MlaA indicate alternative lipoprotein maturation by *N*-palmitoylation and the attachment of two shorter diacylglycerols to the thiol, 33:1 and 32:1, respectively (*SI Appendix*, Fig. S9).

To further confirm our assignment of the $OmpF_3$–MlaA complex, we attempted to sequence the individual subunits using native top–down mass spectrometry. First, we selected peaks assigned to the OmpF trimer and directly fragmented the complex using HCD. Upon collisional activation, we observed sequence ions corresponding with fragmentation of the $OmpF_3$ backbone on surfaces close to the intersubunit interfaces. Next, we fragmented the $OmpF_3$–MlaA complex and noted that fragmentation close to the OmpF interfaces is abolished when MlaA is associated with the trimeric complex (Fig. 4*B*). Rather, $OmpF_3$ in complex with MlaA promotes fragmentation at the inward-facing surfaces of the trimer. We assume that the distribution of mobile protons that drive fragmentation is perturbed in the asymmetric $OmpF_3$–MlaA complex, whereby MlaA might be expected to reduce the charge density in its close vicinity. This top–down experiment confirms the identity of our complex and is consistent with crystal structures of $OmpF_3$–MlaA orthologs from *Klebsiella pneumoniae* and *Serratia marcescens* (9), structure prediction by AlphaFold 3, as well as crosslinking experiments (10).

MlaA was not observed to copurify with lipids and has thus far not been observed to bind phospholipids (1). To study lipid binding to $OmpF_3$–MlaA, we incubated the protein complex with synthetic phospholipids and quantified lipid-bound states by native MS. Incubation of $OmpF_3$–MlaA with DOPG [PG 18:1(9*Z*)/18:1(9*Z*)] led to extensive lipid binding in positive ion mode (Fig. 4*C*). This binding is transient, however, as exchange into lipid-free buffer removed bound phospholipids readily (*SI Appendix*, Fig. S10). Closer inspection of the mass spectrum showed that phospholipid binding increases linearly with the number of MlaA molecules bound to OmpF. Thus, we concluded that MlaA recruits phospholipids to the outer membrane protein complex.

Beyond recruiting lipids, MlaA could also select for specific lipids that are transferred to MlaC. To test whether MlaA shows preferences for certain phospholipids, we incubated $OmpF_3$–MlaA with phospholipids with varying headgroups and lipid chains (Fig. 4*D*) The degree of binding was significantly influenced by the lipid headgroup, ion polarity, and other MS conditions (32). We found that PE and PG bind with similar abundance in the positive mode. Binding of phosphatidylcholine (PC), a major phospholipid in eukaryotes which is not present in *E. coli* membranes, is comparatively low. The trend is reversed in the negative ion mode: DOPC binds with high affinity to $OmpF_3$ and $OmpF_3$–MlaA, whereas PG binding is only observed in the presence of MlaA under these conditions. The observation that MlaA enhances binding of DOPC to the OmpF complex, in both ion polarities, contradicts theoretical simulations which suggested that MlaA does not interact with PCs (9). DOPE binds with intermediate affinity, and its binding is strongly increased by MlaA. Overall, the binding affinities of phospholipids to

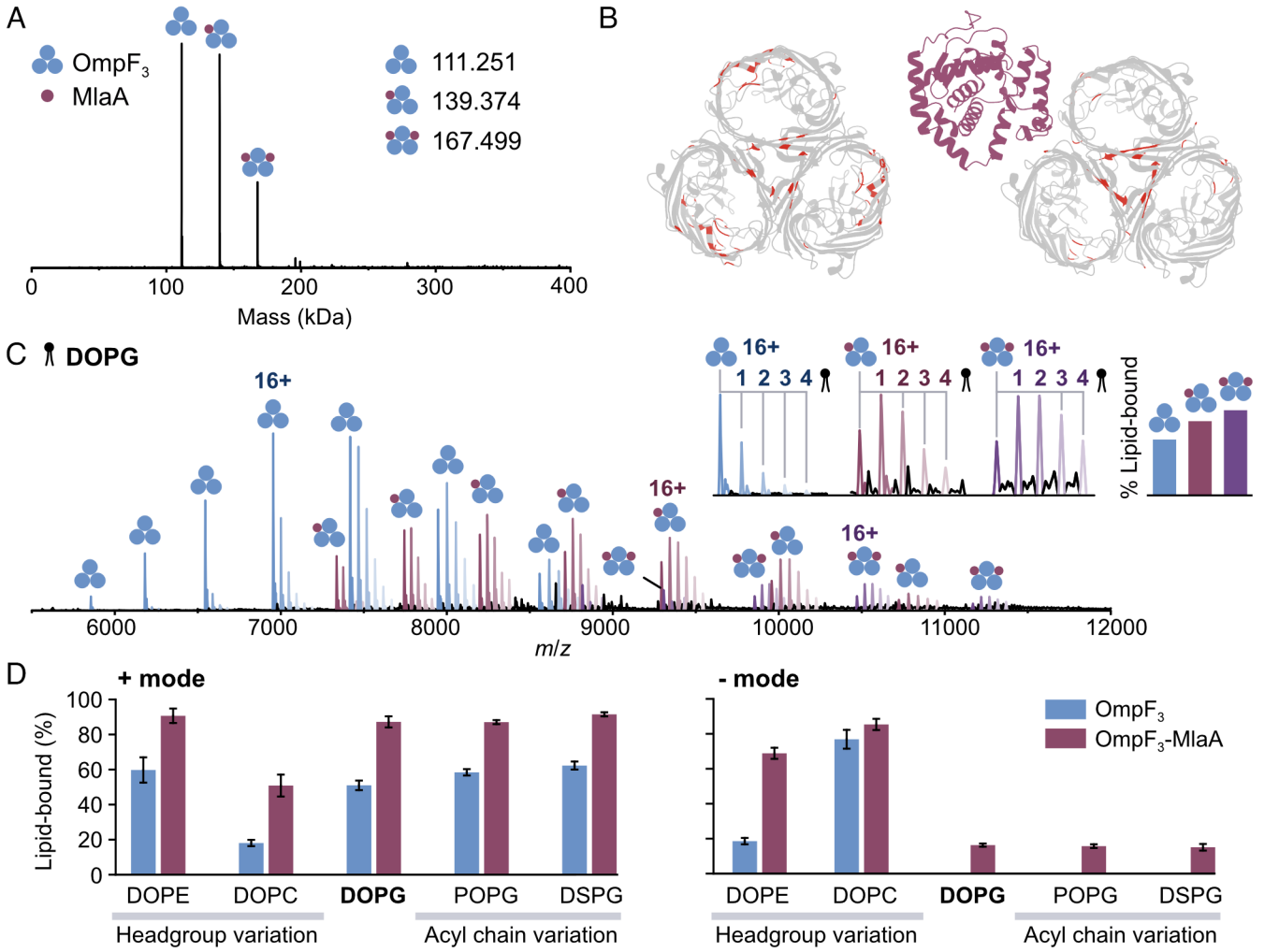

Fig. 4. MlaA recruits lipids to the $OmpF_3$–MlaA complex. (*A*) The deconvolved mass spectrum of MlaA contains three species: $OmpF_3$, $OmpF_3$–MlaA, and $OmpF_3$–$MlaA_2$. (*B*) AlphaFold structures of $OmpF_3$ and $OmpF_3$–MlaA with observed fragmentation sites highlighted in red. (*C*) Native mass spectrum of $OmpF_3$–MlaA incubated with DOPG. With increasing numbers of MlaA molecules bound to $OmpF_3$ (0 to 2), phospholipid binding to the outer membrane protein complex increases. (*D*) Bar charts showing the degree of phospholipid binding to $OmpF_3$ and $OmpF_3$–MlaA for different lipid classes and acyl chains. Lipid binding is mainly determined by the phospholipid headgroup and ion polarity. Error bars represent the SD between triplicate measurements.

$OmpF_3$ and $OmpF_3$–MlaA depend on the ion polarity and charge of the lipid headgroup with no lipid chain-specificity: Varying the degree of saturation (DSPG) or length (POPG) of the lipid chains does not influence their binding affinity to MlaA. We conclude that MlaA binds to all phospholipids investigated, supporting the hypothesis that MlaA does not preselect specific lipids for loading onto MlaC.

MlaA-Mediated Phospholipid Loading of MlaC Shows Preferences. Next, we set out to investigate MlaA-mediated phospholipid loading of MlaC and identify any phospholipid preferences of MlaC in vitro. Accordingly, we incubated delipidated MlaC with different phospholipids at 5-fold molar excess in detergent-containing solution (2xCMC C8E4 in 200 mM ammonium acetate, pH 7.0) (Fig. 5*A*). After 5 min, excess lipids were removed by buffer exchange into detergent-free ammonium acetate before analysis by native MS. While spontaneous loading of *apo* MlaC with phospholipids from liposomes occurs over very long timescales (5, 12), we observed ca. 5% of MlaC loaded with DOPG after 5 min incubation in detergent solution (Fig. 5*B*). To investigate the role of MlaA in this loading process, we repeated the experiment with catalytic concentrations of $OmpF_3$–MlaA. Upon the addition of $OmpF_3$–MlaA the ratio of DOPG-bound MlaC increased by almost one order of magnitude to ~40% (Fig. 5*B*). $OmpF_3$–MlaA thus significantly enhances transfer of DOPG to MlaC compared to passive phospholipid diffusion.

To ascertain that the observed increase in lipid loading in the presence of $OmpF_3$–MlaA is a result of lipid transfer through the MlaA channel into the MlaC binding pocket, rather than resulting from nonspecific lipid scavenging by MlaC at the hydrophobic surfaces of the membrane protein complex, we tested two MlaA mutants, called hereafter MlaA* and MlaA(3G3P). MlaA* is a well-described deletion mutant (ΔAsn41-Phe42), which causes severe phospholipid accumulation in the outer leaflet of the outer membrane (33). Phospholipids from the inner leaflet can access the tunnel of MlaA*, which short-circuits phospholipid transport (9). Accordingly, retrograde phospholipid transport is abolished (5). The second mutant, MlaA(3G3P), results from replacement of three glycines by prolines (141GVGYG → 141PVPYP), which rigidify the linker between a critical hairpin loop and the rest of MlaA (10). MlaA(3G3P) is a loss-of-function mutant which results in a similar phenotype as MlaA knockout. It has been proposed that the mutation locks the adjacent hairpin loop in a closed state that prevents phospholipid transport (10). Importantly, while the mutations in MlaA* and MlaA(3G3P) render MlaA unresponsive to the presence of MlaC and thus abolish retrograde

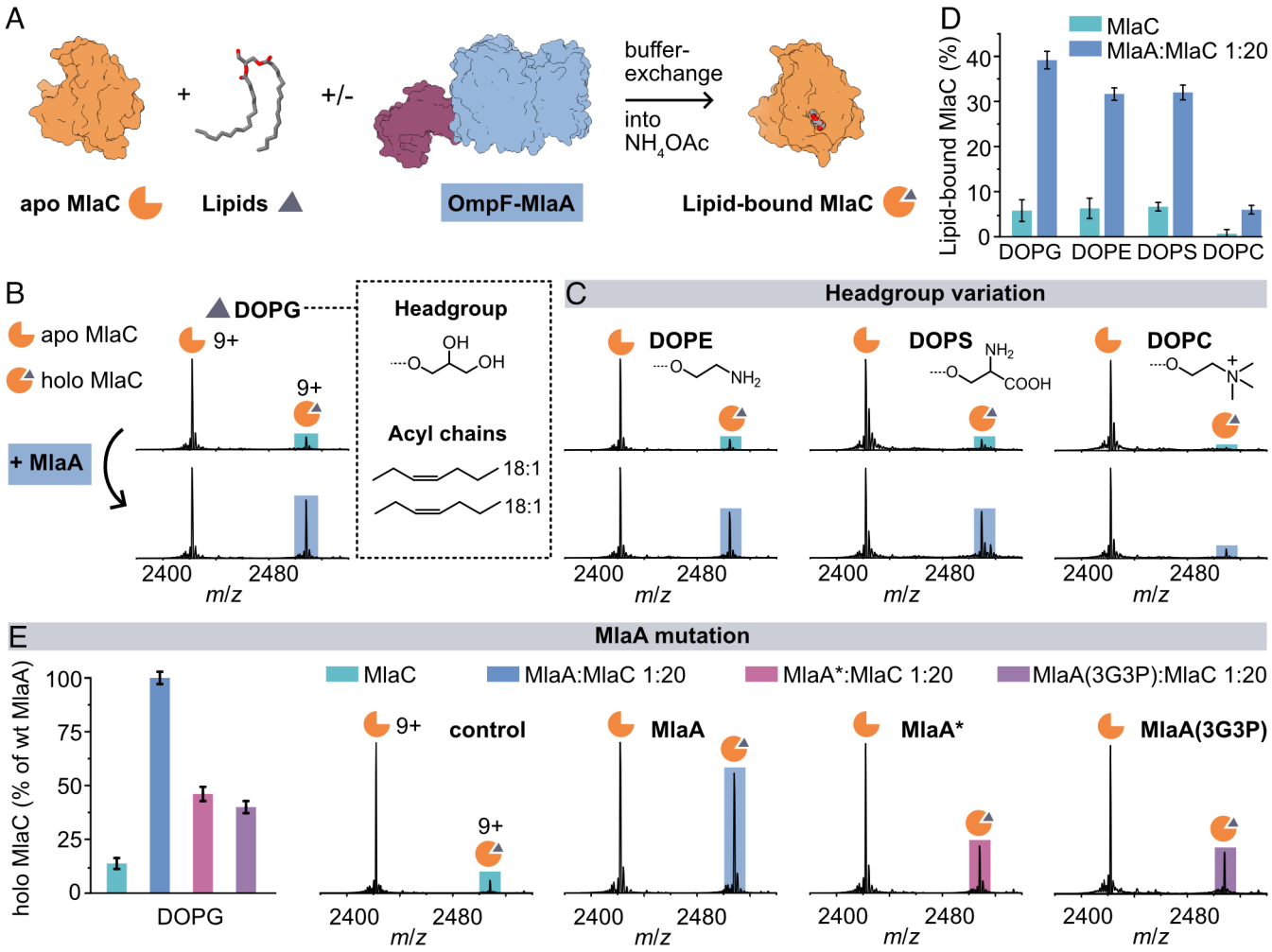

Fig. 5. Loading of delipidated MlaC with synthetic phospholipids in the presence or absence of $OmpF_3$–MlaA. (*A*) Overview of the experiment: MlaC is incubated with lipids with or without adding $OmpF_3$–MlaA in ammonium acetate with 2xCMC C8E4. After buffer exchange into ammonium acetate, the ratio of lipid-loaded MlaC is determined by native MS. (*B*) Loading of MlaC with DOPG is significantly increased in the presence of $OmpF_3$–MlaA. (*C*) DOPE and DOPS bind with similar affinity as DOPG, whereas the binding affinity of DOPC is low. (*D*) Bar chart showing the ratios of lipid-bound MlaC for different phospholipid classes in the presence and absence of $OmpF_3$–MlaA. (*E*) The MlaA mutants MlaA* and MlaA(3G3P) show reduced lipid loading compared to wild type MlaA but increased loading compared to the MlaC-only control. Error bars represent the SD between triplicate measurements.

phospholipid transport (22), they do not affect its association with outer membrane porins (10).

We expressed MlaA* and MlaA(3G3P) under the same conditions as wild type MlaA and confirmed their identity and association with OmpF by native mass spectrometry (*SI Appendix*, Fig. S11). We then repeated the in vitro lipid loading assay with MlaA, MlaA*, and MlaA(3G3P) (Fig. 5*E*). To obtain homogenous samples, we preincubated *apo* MlaC and DOPG, before aliquoting the solution into four tubes to which buffer solution (control), MlaA, MlaA*, or MlaA(3G3P) were added at equal protein concentrations and volumes. After buffer exchange, we observed ca. 5% lipid-bound MlaC in the control sample vs. 50% lipid-bound MlaC in the presence of wild type MlaA, in line with the previous results. Compared to wild type MlaA, lipid loading is reduced by more than half to 20% in the samples containing MlaA* or MlaA(3G3P). These nonfunctional mutants thus have a lower transfer efficiency than wild type MlaA but are able to increase lipid loading three to fourfold compared to passive phospholipid diffusion in the control experiment. This suggests that nonspecific lipid transfer could be facilitated at the MlaA surface. However, the extent of lipid loading is much lower for the mutants than the increase in lipid loading observed for wild type MlaA. The results therefore support the proposal that the reconstituted $OmpF_3$–MlaA–MlaC lipid shuttle accounts for >50% of the observed lipid loading, which results from complex formation and lipid transfer through the MlaA tunnel rather than nonspecific lipid scavenging.

To determine whether MlaC exhibits preferences toward certain phospholipid classes, we endeavored to study solution-phase equilibria between lipid micelles and lipids binding to MlaC for PE, phosphatidylserine (PS), PC, and CDL (Fig. 5*C*). CDL loading was not detected, in accord with the prediction that the binding pocket of *E. coli* MlaC can only accommodate two acyl chains (*SI Appendix*, Fig. S12). DOPG, DOPE, and DOPS were observed to bind to MlaC at very similar levels. Accordingly, MlaC showed no preference for either PE or PG when incubated with *E. coli* lipid extract in the presence of MlaA, independent of the detergent used (*SI Appendix*, Fig. S13). MlaA thus does not preselect PG in vitro, which could have explained the enrichment of PG on endogenous MlaC. In contrast to the major *E. coli* lipids, binding of DOPC is relatively low, even in the presence of MlaA. This was reproduced in a second detergent (DDM) and in the absence of detergent; in both cases, DOPC binding was not detected (*SI Appendix*, Fig. S14). The diminished loading efficiency of PC compared with PE and PG is intriguing, since the headgroup moiety beyond the phosphate that determines the lipid class, does not interact with MlaC in the X-ray crystal structure (14). This would

imply that MlaC should bind to phospholipids without headgroup specificity.

To investigate whether the diminished loading efficiency of PC compared with PG is based on weaker protein–lipid interactions, we performed MD simulations of MlaC in complex with DOPC and DOPG. First, we generated structures of MlaC loaded with DOPC or DOPG based on a crystal structure of lipid-bound MlaC (5UWA) (14). We then simulated the protein–lipid complex in an aqueous solution and derived average protein–lipid distances over 3 μs. We did not observe significant differences between the average distances of DOPC and DOPG from the MlaC binding pocket, suggesting that both protein–lipid complexes are stable in solution (*SI Appendix*, Fig. S19).

We next hypothesized that the reduced loading efficiency of DOPC is not caused by the complex stability itself, but rather by elevated energy barriers in the loading process. We hence performed umbrella sampling to calculate the free energy profiles corresponding to the insertion of DOPG and DOPC into the MlaC binding pocket. The results suggest that there is no apparent energy barrier for phospholipid transfer from solution into the MlaC binding pocket. Nonetheless, the free energy profiles show that the stabilization of DOPG in the MlaC–DOPG complex is increased by ca. 10 kJ mol^{-1} relative to the MlaC–DOPC complex (*SI Appendix*, Fig. S21). Furthermore, the width of the minimum in the free energy profile of phospholipid loading extends further from MlaC in the case of DOPG compared to DOPC, thus implying that DOPG may exhibit a greater preference for loading than DOPC at greater distances from MlaC. Overall, the results suggest that the equilibrium between phospholipid in solution and MlaC–lipid complexes is shifted more toward the MlaC–lipid complex for DOPG than it is for DOPC.

An additional experimental factor that could favor the formation of MlaC–DOPG complexes is the higher expected availability of free DOPG than DOPC in solution: PGs have a lower tendency to form micelles than PCs, and hence more DOPG monomers should be available to MlaC (34). The energy barrier for lipid loading could arise from the need to extract single lipids from micelles. Accordingly, MlaA should accelerate the process by providing a hydrophobic channel and preventing the need for a fully solvated lipid. Regardless of the different solution-phase equilibria for different phospholipid classes, our results clearly demonstrate that the addition of $OmpF_3$–MlaA increases loading significantly for all phospholipids investigated (Fig. 5*D*).

Assembly and Dissociation of the Transient $OmpF_3$–MlaA–MlaC Complex. Finally, we set out to capture the elusive $OmpF_3$–MlaA–MlaC complex and track the individual steps of MlaA-mediated lipid transfer by native MS. First, we incubated $OmpF_3$–MlaA and delipidated MlaC at a 1:1 ratio in 200 mM ammonium acetate containing 2xCMC C8E4. The addition of *apo* MlaC to $OmpF_3$–MlaA led to the formation of a new species corresponding to the ternary $OmpF_3$–MlaA–MlaC(*apo*) complex (Fig. 6 *A* and *B*). The formation of $OmpF_3$–MlaC complexes was not observed, which demonstrates that MlaC specifically binds to the MlaA portion of the outer membrane protein complex, as previously suggested by crosslinking experiments (22).

To observe the impact of phospholipid binding on the stability of the $OmpF_3$–MlaA–MlaC complex we added PG 36:2 (DOPG) to the assembly and recorded a mass spectrum immediately after lipid addition (Fig. 6*C*). Adding DOPG to the protein assemblies led to a decrease of the $OmpF_3$–MlaA–MlaC(*apo*) complex (P = 0.001; *SI Appendix*, Fig. S16). At the same time, DOPG-loaded MlaC became apparent in the lower mass range of the same spectrum. Because the presence of detergent impeded quantification of lipid-bound MlaC, we buffer-exchanged the sample into ammonium acetate and found that ca. 20% of MlaC was bound to DOPG after 5 min incubation (*SI Appendix*, Fig. S16). We also observed lipid binding to both $OmpF_3$–MlaA and $OmpF_3$–$MlaA_2$, but no lipid-bound $OmpF_3$–MlaA–MlaC complex. Although we cannot exclude that lipid-bound peaks are not apparent due to the low abundance of the ternary complex, this finding is in line with the suggestion that lipid-bound $OmpF_3$–MlaA–MlaC complex is unstable (22). We infer that the protein complex dissociates after phospholipid transfer from MlaA to MlaC, releasing $OmpF_3$–MlaA and lipid-bound MlaC. In sum, we were able to capture the transient ternary $OmpF_3$–MlaA–MlaC(*apo*) complex and observe its dissociation upon lipid transfer to MlaC. Thus, we reconstituted the lipid shuttle, with the preferred MlaC lipid, in solution and captured all essential steps of MlaA-mediated phospholipid transfer to MlaC by native MS.

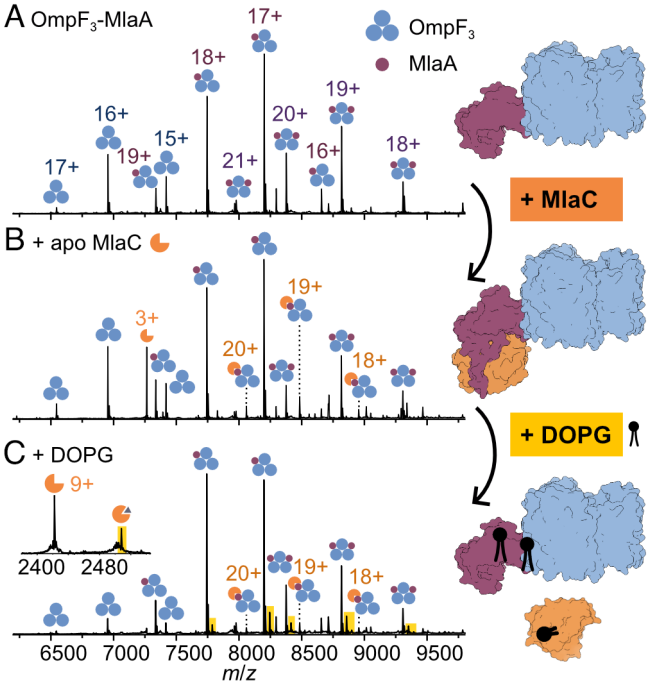

Fig. 6. Formation and dissociation of the transient $OmpF_3$–MlaA–MlaC(*apo*) complex captured by native MS. (*A*) The native mass spectrum of purified MlaA contains three species: OmpF, $OmpF_3$–MlaA, and $OmpF_3$–$MlaA_2$. (*B*) Addition of *apo* MlaC leads to the emergence of the ternary $OmpF_3$–MlaA–MlaC(*apo*) complex. (*C*) The protein complex partially dissociates when DOPG is added, releasing lipid-bound MlaC (*Inset* shown after detergent removal). DOPG also binds to $OmpF_3$–MlaA and $OmpF_3$–$MlaA_2$ (yellow). Protein complex cartoons were generated using AlphaFold3.

Discussion

In this study, we characterized the endogenous lipids transported by the bacterial phospholipid transporter MlaC, and studied phospholipid transfer from MlaA to MlaC in solution using native MS. We demonstrate that MlaC expressed under native conditions copurifies with a three-fold enrichment of PG compared to the whole-cell PG content. We could not relate this finding to a preference of MlaC for PG or selectivity of MlaA toward PG in vitro, suggesting that this enrichment is unique to the cellular environment.

There are several possible reasons why we observe an enrichment of PG on endogenous MlaC. Assuming that MlaC receives phospholipids from the outer leaflet of the outer membrane, the accumulation could result from a higher tendency of PG to flip across the outer membrane. In the current absence of studies on lipid flipping at the bacterial outer membrane, this is difficult to estimate, as the flipping propensity is highly dependent on the

membrane composition and cannot be derived from experiments on simple model membranes (28). Due to their negative charge at neutral pH, however, PG should be less prone to flipping than zwitterionic PE (29). On the other hand, it was shown that membrane-spanning domains of proteins can catalyze lipid flipping and accelerate the flipping of PG substantially over PE (30).

Another explanation for the observed enrichment of PG could be that alternative mechanisms exist that remove PE from the outer leaflet of the outer membrane. The outer membrane proteins PagP and PldA degrade phospholipids by removing fatty acids (1). However, PE and PG are both comparably efficient substrates of PagP (31, 32), and PldA mutations do not alter the phospholipid composition (33), pointing toward little or no phospholipid selectivity of the two enzymes. Nonetheless, there might be other yet unknown pathways that degrade or remove PE from the outer leaflet of the outer membrane. Alternatively, it is also possible that MlaFEDB unloads PE more efficiently than PG at the inner membrane, resulting in a net enrichment of PG on MlaC.

Interestingly, PG has also been found to be enriched on overexpressed MlaD (35), which could be a direct result of increased PG transport through the Mla system. On the other hand, the finding that MlaC overexpressed in the cytosol is enriched in PG is surprising, as it can neither be loaded nor unloaded by the other Mla components in vivo (18). However, one can wonder in general how cytoplasmic MlaC, which copurified with a large amount of phospholipids, was loaded with lipids at all. Our experiments together with those reported previously (12) showed that loading of MlaC by lipid diffusion in solution is negligible. On the other hand, short contact with catalytic amounts of MlaA increases lipid loading to a great extent. Hence, it is possible that MlaC overexpressed in the cytosol is loaded during high pressure lysis, which mixes the membranes and enables contact between MlaC and MlaA.

In addition to characterizing the lipids transported by MlaC, we reconstructed the $OmpF_3$–MlaA–MlaC lipid shuttle in solution. We observed that MlaA recruits phospholipids to OmpF, likely providing a pool of phospholipids close to the channel entrance which could be readily passaged through the channel to MlaC. $OmpF_3$–MlaA significantly increased loading of different phospholipid classes onto MlaC compared to nonfunctional MlaA mutants or passive phospholipid diffusion in solution. We dissected the loading process into two steps: formation of the transient $OmpF_3$–MlaA–MlaC complex and dissociation of lipid-bound MlaC from the complex upon addition of PG. We thus showed that the transient $OmpF_3$–MlaA–MlaC complex could be captured and investigated by native MS. Overall therefore we have elucidated and reconstituted a crucial process occurring at the outer membrane of gram-negative bacteria, essential for both membrane integrity and antibiotic resistance.

Materials and Methods

Recombinant Protein Expression. MlaC and MlaA were expressed and purified according to reported protocols with minor modifications (12, 14). Codon-optimized DNA corresponding to MlaC with N-terminal signal peptide followed by a hexahistidine tag and TEV protease cleavage site was cloned by Gibson assembly into a pET28b vector. Codon-optimized DNA corresponding to full-length MlaA, MlaA* (ΔAsn41-Phe42), and MlaA(3G3P) (141GVGYG → 141PVPYP) were cloned into pET15 vectors resulting in a TEV protease cleavage site and C-terminal hexahistidine tag. *E. coli* BL21(DE3) (New England Biolabs) cells were cotransformed with the MlaC- and MlaA-encoding plasmids under kanamycin (50 μg/mL) and ampicillin (100 μg/mL) selection, and separately transformed with the plasmids encoding MlaA and MlaA mutants under ampicillin selection. MlaC co-overexpressed with MlaA was made and purified in triplicate, starting from different colonies. Overnight cultures were grown with shaking in Luria Broth (LB) under the respective antibiotic selection at 37 °C. 10 mL of the overnight cultures was used to inoculate 1 L of expression culture. The cultures were grown at 37 °C to OD_{600} = 0.5 and then cooled before IPTG was added to a final concentration of 0.8 mM. Protein expression was performed at 16 °C for 5 h for MlaA and MlaA mutants and overnight for MlaC. Cell pellets were harvested by centrifugation at 5000 × *g* for 15 min. Proteins were purified by affinity chromatography as detailed in the *SI Appendix, Extended Methods*.

Stepwise Delipidation of MlaC. MlaC was delipidated following a reported protocol with slight modifications ($n = 3$, different days) (12). Purified, His-tagged MlaC was loaded onto four 0.5-mL Ni-NTA affinity columns equilibrated with wash buffer (50 mM Tris pH 8.0, 300 mM NaCl, 10 mM imidazole). The columns were washed with 5 CV wash buffer, before being filled with 5 CV delipidation buffer (50 mM Tris pH 8.0, 300 mM NaCl, 10 mM imidazole, 2% OG) and placed on a roller for 1 h. MlaC was eluted from the first column with 5 CV elution buffer (50 mM Tris pH 8.0, 300 mM NaCl, 300 mM imidazole), while fresh delipidation buffer was added to the remaining columns and the process was repeated. MlaC was eluted from the first three columns after one, two, and three 1 h delipidation steps. The fourth sample was eluted after a fourth delipidation step overnight. The elutions were dialyzed against dialysis buffer (50 mM Tris pH 8.0, 150 mM NaCl) and concentrated. All steps were performed at 4 °C.

Endogenous Tagging and Purification of MlaC. *E. coli* MlaC was endogenously tagged with an N-terminal Twin-Strep tag after the signal sequence using lambda Red recombination (28). The fusion allele was transduced into *E. coli* wild type strain BW25113 by P1 phage transduction (29). After removal of the kanamycin cassette using the pCP20 plasmid, cells were grown to an OD_{600} of 0.7 to 0.8 and pelleted. Cells were lysed by hypotonic lysis and purified by using Strep-TactinXT 4Flow High Capacity resin (IBA Lifesciences), as detailed in the *SI Appendix, Extended Methods*.

Mass Spectrometry. Two different mass spectrometers were employed in this study: a Q-Exactive UHMR mass spectrometer (ThermoFisher Scientific) for native MS analysis, and an Orbitrap Eclipse Tribrid mass spectrometer (ThermoFisher Scientific) for bound lipid identification, native top–down MS, and lipidomics. Capillaries for nano electrospray ionization were pulled in-house using a P97 Micropipette Puller (Sutter Instrument Corporation), and coated with gold by an Agar Auto Sputter Coater. The respective instrument parameters are specified in the *SI Appendix, Extended Methods*, and raw spectra are accessible via Figshare (36).

Loading of MlaC with Phospholipids. To load MlaC with synthetic lipids in detergent, 5 μM delipidated MlaC was added to a solution of 25 μM (final concentration) phospholipids in 200 mM ammonium acetate (pH 7.0) with 2xCMC C8E4 and either 0.25 μM or no $OmpF_3$–MlaA. Loading of MlaC with natural *E. coli* lipid extract was achieved analogously using a total lipid concentration of ca. 750 μM. The effect of $OmpF_3$–MlaA on lipid loading was found to saturate above an MlaA:MlaC ratio of 1:50 (corresponding to a concentration of 0.1 μM $OmpF_3$–MlaA); *SI Appendix*, Fig. S15. For loading experiments with MlaA mutants, $OmpF_3$–MlaA, $OmpF_3$–MlaA*, and $OmpF_3$–MlaA(3G3P) were buffer-exchanged into 200 mM ammonium acetate with 2xCMC C8E4 and diluted to equal concentration (ca. 10 μM). Equal volumes of $OmpF_3$–MlaA and mutants (0.25 μM final concentration) were then added in separate tubes to a mixture of *apo* MlaC (5 μM final concentration) and DOPG (25 μM final concentration) in 200 mM ammonium acetate with 2xCMC C8E4. To ensure homogenous conditions, MlaC and DOPG were mixed before aliquoting into the individual test tubes. This solution containing only MlaC and DOPG in detergent buffer further served as control sample. The solutions were vortexed and incubated without agitation for 5 min. 20 μL of each solution was buffer-exchanged into 200 mM ammonium acetate using BioSpin-6 columns (BioRad) to remove excess lipids. The buffer-exchanged samples were measured without dilution on the UHMR Q-Exactive mass spectrometer.

MD Simulations. MD simulations were performed using GROMACS version 2022.5 (37). Input structures were generated based on a crystal structure of diacylglycerol-bound MlaC (5UWA) (14) by removing the second MlaC molecule (chain B) and water molecules and replacing the diacylglycerol ligand with DOPG or DOPC. GROMACS input files were generated with CHARMM-GUI (38, 39) using the Charmm36 force field (40) and TIP3P water model (41, 42). Protein dynamics were simulated for a total simulation time of 3 μs. Umbrella sampling

was performed for MlaC in complex with DOPG and DOPC. Computational details are described in the *SI Appendix, Extended Methods*.

Data, Materials, and Software Availability. Raw data underlying the Figures shown in the main text and *SI Appendix* have been deposited on Figshare (DOI: 10.25446/oxford.28590011) (36). Code critical to the findings of this manuscript is available at https://github.com/kanalstrahlen/MS2toMS1fitter/ (26). All other data are included in the article and/or *SI Appendix*.

ACKNOWLEDGMENTS. This work was supported by a Wellcome Trust grant (221795/Z/20/Z; C.V.R.) and the Leopoldina fellowship program of the German National Academy of Sciences Leopoldina (LPDS 2023-07; C.K.). Q.T. acknowledges funding by the CIU trust. G.I. holds an MRC career development award (MR/W016672/1). I.P.S.S. is funded through HECBioSim (EP/X035603). S.K. is funded by EPSRC Grants EP/X035603 and EP/V030779/1. This work used the ARCHER2 UK National Supercomputing Service. We thank Prof. Stephan Uphoff for providing the MlaC knockout strain.

Author affiliations: [a]Kavli Institute for Nanoscience Discovery, University of Oxford, Oxford OX1 3QU, United Kingdom; [b]Department of Chemistry, University of Oxford, Oxford OX1 3QU, United Kingdom; [c]Sir William Dunn School of Pathology, University of Oxford, Oxford OX1 3RE, United Kingdom; and [d]Department of Biochemistry, University of Oxford, Oxford OX1 3QU, United Kingdom

1. E. Lundstedt, D. Kahne, N. Ruiz, Assembly and maintenance of lipids at the bacterial outer membrane. *Chem. Rev.* **121**, 5098–5123 (2021).
2. J. E. Horne, D. J. Brockwell, S. E. Radford, Role of the lipid bilayer in outer membrane protein folding in Gram-negative bacteria. *J. Biol. Chem.* **295**, 10340–10367 (2020).
3. Y. Takeuchi, H. Nikaido, Persistence of segregated phospholipid domains in phospholipid–lipopolysaccharide mixed bilayers: Studies with spin-labeled phospholipids. *Biochemistry* **20**, 523–529 (1981).
4. J. C. Malinverni, T. J. Silhavy, An ABC transport system that maintains lipid asymmetry in the gram-negative outer membrane. *Proc. Natl. Acad. Sci. U.S.A.* **106**, 8009–8014 (2009).
5. X. Tang *et al.*, Structural insights into outer membrane asymmetry maintenance in Gram-negative bacteria by MlaFEDB. *Nat. Struct. Mol. Biol.* **28**, 81–91 (2021).
6. J. Abellon-Ruiz, Forward or backward, that is the question: Phospholipid trafficking by the Mla system. *Emerg. Top. Life Sci.* **7**, 125–135 (2023).
7. W. Y. Low, S. S. Chng, Current mechanistic understanding of intermembrane lipid trafficking important for maintenance of bacterial outer membrane lipid asymmetry. *Curr. Opin. Chem. Biol.* **65**, 163–171 (2021).
8. Z. S. Chong, W. F. Woo, S. S. Chng, Osmoporin OmpC forms a complex with MlaA to maintain outer membrane lipid asymmetry in Escherichia coli. *Mol. Microbiol.* **98**, 1133–1146 (2015).
9. J. Abellon-Ruiz *et al.*, Structural basis for maintenance of bacterial outer membrane lipid asymmetry. *Nat. Microbiol.* **2**, 1616–1623 (2017).
10. J. Yeow *et al.*, The architecture of the OmpC-MlaA complex sheds light on the maintenance of outer membrane lipid asymmetry in Escherichia coli. *J. Biol. Chem.* **293**, 11325–11340 (2018).
11. B. Ercan, W. Y. Low, X. Liu, S. S. Chng, Characterization of Interactions and Phospholipid Transfer between Substrate Binding Proteins of the OmpC-Mla System. *Biochemistry* **58**, 114–119 (2019).
12. G. W. Hughes *et al.*, Evidence for phospholipid export from the bacterial inner membrane by the Mla ABC transport system. *Nat. Microbiol.* **4**, 1692–1705 (2019).
13. V. K. James, B. J. Voss, A. Helms, M. S. Trent, J. S. Brodbelt, Investigating lipid transporter protein and lipid interactions using variable temperature electrospray ionization, ultraviolet photodissociation mass spectrometry, and collision cross section analysis. *Anal. Chem.* **96**, 12676–12683 (2024).
14. D. C. Ekiert *et al.*, Architectures of Lipid Transport Systems for the Bacterial Outer Membrane. *Cell* **169**, 273–285 e217 (2017).
15. D. Yero *et al.*, The Pseudomonas aeruginosa substrate-binding protein Ttg2D functions as a general glycerophospholipid transporter across the periplasm. *Commun. Biol.* **4**, 448 (2021).
16. M. R. MacRae *et al.*, Protein-protein interactions in the Mla lipid transport system probed by computational structure prediction and deep mutational scanning. *J. Biol. Chem.* **299**, 104744 (2023).
17. D. C. Ekiert, N. Coudray, G. Bhabha, Structure and mechanism of the bacterial lipid ABC transporter, MlaFEDB. *Curr. Opin. Struct. Biol.* **76**, 102429 (2022).
18. W. Y. Low, S. Thong, S. S. Chng, ATP disrupts lipid-binding equilibrium to drive retrograde transport critical for bacterial outer membrane asymmetry. *Proc. Natl. Acad. Sci. U.S.A.* **118**, e2110055118 (2021).
19. X. Chi *et al.*, Structural mechanism of phospholipids translocation by MlaFEDB complex. *Cell Res.* **30**, 1127–1135 (2020).
20. P. Wotherspoon *et al.*, Structure of the MlaC-MlaD complex reveals molecular basis of periplasmic phospholipid transport. *Nat. Commun.* **15**, 6394 (2024).
21. M. J. Powers, M. S. Trent, Intermembrane transport: Glycerophospholipid homeostasis of the Gram-negative cell envelope. *Proc. Natl. Acad. Sci. U.S.A.* **116**, 17147–17155 (2019).
22. J. Yeow, M. Luo, S. S. Chng, Molecular mechanism of phospholipid transport at the bacterial outer membrane interface. *Nat. Commun.* **14**, 8285 (2023).
23. F. F. Hsu, J. Turk, Electrospray ionization with low-energy collisionally activated dissociation tandem mass spectrometry of glycerophospholipids: Mechanisms of fragmentation and structural characterization. *J. Chromatogr. B Analyt. Technol. Biomed. Life Sci.* **877**, 2673–2695 (2009).
24. D. Oursel *et al.*, Lipid composition of membranes of Escherichia coli by liquid chromatography/tandem mass spectrometry using negative electrospray ionization. *Rapid Commun. Mass Spectrom.* **21**, 1721–1728 (2007).
25. E. G. Bligh, W. J. Dyer, A rapid method of total lipid extraction and purification. *Can. J. Biochem. Physiol.* **37**, 911–917 (1959).
26. C. Kirschbaum, J. L. Bennett, MS2toMS1fitter. Zenodo. https://doi.org/10.5281/zenodo.15046305. Deposited 18 March 2025.
27. S. Quan, A. Hiniker, J.-F. Collet, J. C. A. Bardwell, "Isolation of bacteria envelope proteins" in *Bacterial Cell Surfaces: Methods and Protocols*, A. H. Delcour, Ed. (Humana Press, 2013), pp. 359–366.
28. K. A. Datsenko, B. L. Wanner, One-step inactivation of chromosomal genes in Escherichia coli K-12 using PCR products. *Proc. Natl. Acad. Sci. U.S.A.* **97**, 6640–6645 (2000).
29. L. C. Thomason, N. Costantino, D. L. Court, E. coli genome manipulation by P1 transduction. *Curr. Protoc. Mol. Biol.* **1**, 18 (2007).
30. A. Skerra, A. Pluckthun, Assembly of a functional immunoglobulin Fv fragment in Escherichia coli. *Science* **240**, 1038–1041 (1988).
31. J. El Rayes, R. Rodriguez-Alonso, J. F. Collet, Lipoproteins in Gram-negative bacteria: New insights into their biogenesis, subcellular targeting and functional roles. *Curr. Opin. Microbiol.* **61**, 25–34 (2021).
32. I. Liko *et al.*, Lipid binding attenuates channel closure of the outer membrane protein OmpF. *Proc. Natl. Acad. Sci. U.S.A.* **115**, 6691–6696 (2018).
33. H. A. Sutterlin *et al.*, Disruption of lipid homeostasis in the Gram-negative cell envelope activates a novel cell death pathway. *Proc. Natl. Acad. Sci. U.S.A.* **113**, E1565–1574 (2016).
34. D. Marsh, *Handbook of Lipid Bilayers* (CRC Press, ed. 2, 2013).
35. S. Thong *et al.*, Defining key roles for auxiliary proteins in an ABC transporter that maintains bacterial outer membrane lipid asymmetry. *Elife* **5**, e19042 (2016).
36. C. Kirschbaum *et al.*, Dataset for "Following phospholipid transfer through the OmpF3–MlaA–MlaC lipid shuttle with native mass spectrometry." Figshare. https://doi.org/10.25446/oxford.28590011. Deposited 18 March 2025.
37. M. J. Abraham *et al.*, GROMACS: High performance molecular simulations through multi-level parallelism from laptops to supercomputers. *SoftwareX* **2**, 19–25 (2015).
38. S. Jo, T. Kim, V. G. Iyer, W. Im, CHARMM-GUI: A web-based graphical user interface for CHARMM. *J. Comput. Chem.* **29**, 1859–1865 (2008).
39. J. Lee *et al.*, CHARMM-GUI input generator for NAMD, GROMACS, AMBER, OpenMM, and CHARMM/OpenMM simulations using the CHARMM36 additive force field. *J. Chem. Theory Comput.* **12**, 405–413 (2016).
40. R. B. Best *et al.*, Optimization of the additive CHARMM all-atom protein force field targeting improved sampling of the backbone phi, psi and side-chain chi(1) and chi(2) dihedral angles. *J. Chem. Theory Comput.* **8**, 3257–3273 (2012).
41. W. L. Jorgensen, J. Chandrasekhar, J. D. Madura, R. W. Impey, M. L. Klein, Comparison of simple potential functions for simulating liquid water. *J. Chem. Phys.* **79**, 926–935 (1983).
42. D. J. Price, C. L. Brooks IIIrd, A modified TIP3P water potential for simulation with Ewald summation. *J. Chem. Phys.* **121**, 10096–10103 (2004).